Time-domain Fresnel-to-Fraunhofer diffraction with photon echoes

Menager, L.; Lorgere, I.; Le Gouet, J; Mohan, R. K.; Kröll, Stefan

Published in:
Optics Letters

1999

Time-domain Fresnel-to-Fraunhofer diffraction with photon echoes

Loïc Ménager, Ivan Lorgeré, and Jean-Louis Le Gouët

Laboratoire Aimé Cotton, Centre National de la Recherche Scientifique II, Bâtiment 505, 91405 Orsay Cédex, France

R. Krishna Mohan and Stefan Kröll

Lund Institute of Technology, Box 118, S-22100 Lund, Sweden

Received March 1, 1999

A photon echo experiment in Tm^{3+}:YAG is reported that shows, for the first time to the authors' knowledge, the time-domain equivalent of the transition from near- to far-field diffraction, including Talbot self-imaging effects. The experiment demonstrates the huge dispersion capability of photon echoes and opens the way to further exploration of space–time duality. © 1999 Optical Society of America

OCIS codes: 190.4380, 070.6760, 070.4790, 200.4740.

Photon echoes in condensed matter at low temperature have proved to be a powerful tool for time-domain optical signal processing.[1–3] Rare-earth-doped crystals are well suited to optical processing of rf signals because they have the ability to process bandwidths in the range of gigahertz to hundreds of gigahertz with a time–bandwidth product well above 10.[4] In addition, thulium- or erbium-doped crystals have absorption lines at wavelengths at which compact laser sources,[4] fast optoelectronic devices, and optical amplifiers[5] are available. Such applications of these crystals as true time-delay generators[2] for phased array antennas and in spectral analysis of rf signals[6] are under study.

Space–time duality[7] gives attractive guidelines for the design of time-domain optical processing schemes. In this duality, temporal dispersion is the equivalent of diffraction, whereas linear chirping provides the time equivalent of a lens. Experimental demonstrations of this duality that have been reported so far have dealt with picosecond laser pulses. A grating pair was used as a dispersive line, and an electro-optic phase modulator[8,9] or an optical nonlinear wave-mixing process[10] as a time lens. The time–bandwidth product of an electro-optic time lens is given by the peak phase deviation of the modulator and is therefore quite poor, below 100, which is not satisfactory for optical signal processing. The alternative approach to creating a time lens based on optical wave mixing in a nonlinear crystal has the potential for a high time–bandwidth product.[10] However, these tools have been designed to deal with terahertz-bandwidth pulses and are inappropriate for processing gigahertz-bandwidth optical signals. In particular, processing a gigahertz bandwidth with a high time–bandwidth product requires a dispersive line that achieves microsecond group delays. In this Letter we show that photon echoes in rare-earth-doped crystals can achieve a flexible dispersive line with incomparable dispersion. An experiment with a thulium-doped YAG crystal is reported, in which the first demonstration to our knowledge is made of the time-domain equivalent of the transition from Fresnel to Fraunhofer diffraction. We conclude by pointing out the time lens that could fit this dispersive line.

The shape of the three-pulse photon-echo signal, built, for instance, on an atomic transition of a rare-earth ion doping a crystal, can be described as[11]

$$E_e(t) = E_1^*(-t) \otimes E_2(t) \otimes E_3(t)\,, \tag{1}$$

where $E_i(t)$ are centered about $t = 0$ and describe the envelopes of the excitation pulses, which are assumed to be temporally separated and with the time order E_1, E_2, E_3; $\otimes$ represents the convolution product. From the point of view of time-domain holography the echo signal is the result of reading with pulse E_3 the spectral hologram engraved in the crystal by the first two pulses. The duration of the recorded shape $E_1^*(-t) \otimes E_2(t)$ is limited by the dephasing time of the atomic transition, and its spectral bandwidth should not exceed the inhomogeneous width of the atomic transition in the host crystal. Equation (1) is readily transformed into a diffractionlike integral. Let E_2 be the input signal and E_1 a short reference pulse such that $E_1^*(-t) \otimes E_2(t) = E_2(t)$. Now let E_3 be a long wideband chirped pulse, that is, a pulse whose spectral bandwidth is given by $r\tau_3$, where r is the chirp rate and τ_3 is the pulse duration. If in addition this bandwidth covers uniformly that of the input signal, such a pulse can be written as $E_3(t) = \exp i\pi r t^2$ in echo expression (1), which then reads as

$$E_e(t) = \int E_2 t' \exp i\pi r(t - t')^2 \mathrm{d}t'. \tag{2}$$

The echo here appears as the result of dispersion of input signal $E_2(t)$: Each frequency component ν is delayed by $T(\nu) = \nu/r$. In this dispersion process the maximum achievable group delay T is limited by the coherence time of the atomic transition. It can therefore be several tens of microseconds in thulium-doped crystals,[12] which is to be contrasted with the 500 ps that a grating pair[13] can typically achieve. This photon-echo process offers matchless group-delay dispersion. In addition, the group-delay dispersion rate $\partial T/\partial \nu$ is given by the inverse chirp rate and can therefore easily be controlled and varied over a broad range.

From the space–time duality point of view, this dispersion process is the time dual of diffraction over a

0146-9592/99/140927-03$15.00/0

distance d, with the equivalence $\lambda d \leftrightarrow 1/r$, where λ is the optical wavelength. Indeed, Eq. (2) also gives, under the Fresnel approximation, the field $E_e(x)$ diffracted at distance d by a one-dimensional aperture with transmission function $E_2(x')$ and illuminated by a plane wave. If τ_2 is the duration of input signal $E_2(t')$, one can define a time-domain Fresnel number $F = r\tau_2{}^2$. As is well known in the space domain, the transition from near- to far-field diffraction is observed for values of the Fresnel number near unity. For $F > 1$ we are in the Fresnel diffraction range, where the diffracted pattern is highly sensitive to variation of the Fresnel number. Interesting effects such as Talbot self-imaging[14] can be observed in this situation. For $F < 1$, the diffracted pattern intensity is given by the Fourier transform of the input field. The chirped photon-echo process described above gives the opportunity to observe this transition in the time domain, which we have verified experimentally.

We performed the experiment illustrated in Fig. 1 on a 0.1-at.% thulium-doped YAG crystal, 5 mm thick, from Scientific Material Corporation. The crystal was immersed in a liquid-helium cryostat and held at ~4 K. The light source was a cw argon-pumped Ti:sapphire laser. The laser frequency, with a linewidth of ~200 kHz, was tuned to 12 604.3 cm^{-1}, the center of the $^3H_6 \rightarrow {}^3H_4$ absorption line of the Tm^{3+} ions. The maximum optical density of the crystal was measured to be ~0.75. The inhomogeneous width of this transition is ~15 GHz. The optical setup was a collinear photon-echo setup. For a better extinction ratio two acousto-optic cells, AO1 and AO2, fed by the same rf driver, were used to modulate in amplitude and frequency the cw laser output. The frequency shifts produced by the two AO cells added together. The cw laser power before the cryostat was 35 mW. The laser spot, ~4 mm in diameter, was focused onto the crystal by 15-cm focal-length lens L1. Under these conditions, $\pi/2$ pulses were achieved with 1.5-μs-long pulses. The echo signal was detected with photomultiplier tube PM through acousto-optic gate AO3, which was used to reject the excitation pulses.

For the diffractionlike experiments, first the sample was excited by a 1.5-μs-long train of eight 80-ns-long pulses separated by 200 ns. The second excitative pulse, E_2, was an identical train, delayed 15 μs with respect to the first. The duration of this exciting sequence was therefore less than the dephasing time of the transition, which we measured to be ~30 μs. Reading pulse E_3 was a 12-μs-long pulse, with a linear chirp controlled by means of the driving frequency of acousto-optic modulators AO1 and AO2. With this excitation scheme the echo can be described by Eq. (2), provided that $E_2(t)$ is replaced by the autocorrelation $E_2{}^*(-t) \otimes E_2(t)$ because E_1 is not a short pulse but is instead a replica of pulse E_2. It is the limited laser power that prevented us from making E_1 a short pulse. The echo is therefore the result of dispersion of the pulse-train autocorrelation function, which is the input signal to be considered. Figure 2(a) displays the square of its theoretical profile.

The echo signal power $|E_e t|^2$ was recorded for different values of the chirp rate that ranged from 1.1 to 4.55 MHz/μs. The records are displayed in Fig. 3 together with the results of simulation with Eq. (2). As can be seen, there is good agreement between the experimental results and the simulations. The only fitting parameter in the simulation was the chirp-rate value. Minor deviations of <10% from the experimental chirp-rate values were necessary for optimal fit. Observation of Figs. 3(a) and 3(b) shows that the amplitude of the oscillations is smaller on the experimental traces than on the simulations. Shot-to-shot fluctuations of the temporal position of the echo signal may explain this difference, since experimental traces a and b result from averages over 4 and 64 shots, respectively. These fluctuations can arise from jitter on the delay between the first and second pulse trains and from laser frequency instabilities. More disconcerting is the phase difference between the experimental and the simulated oscillations in Fig. 3(b). More research is necessary to explain the latter discrepancy.

Figure 2 shows for reference the squares of the theoretical pulse-train autocorrelation function and power spectrum. These are the expected echo shapes for infinitely high and low chirp rates, respectively, which are time duals of diffraction over zero and infinite distance. The experimental records show the transition between these two situations. Indeed, one can clearly identify in Figs. 3(a) and 3(b) the periodic peaks whose 200-ns period is that of the pulse train and that are inscribed under a bell-shaped envelope. The recordings of Figs. 3(c) and 3(d) show the three distinct peaks that are characteristic of the pulse-train power spectrum. The time-domain Fresnel number $r\tau_2{}^2$ for these records ranges from 2.5 to 10. This means that

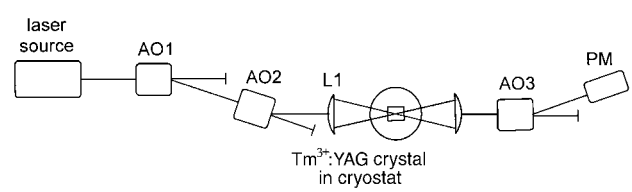

Fig. 1. Experimental setup.

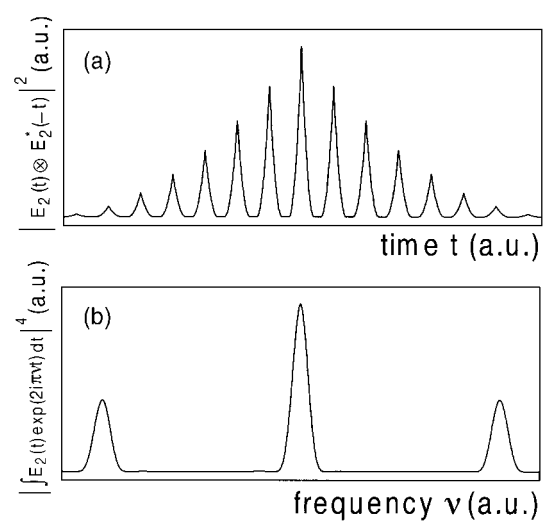

Fig. 2. Theoretical profiles of the square of the (a) autocorrelation function and (b) power spectrum of the input pulse train, assuming square pulses.

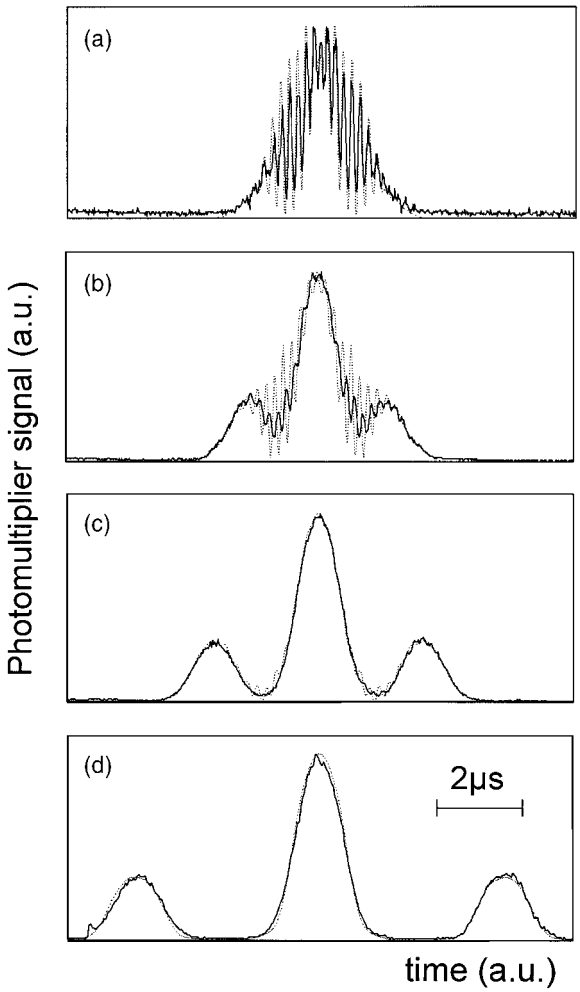

Fig. 3. Temporal shape of photon-echo power for the following chirp-rate values of r: (a) 4.55, (b) 3.1, (c) 2, (d) 1.1 MHz/μs. Continuous curves, experimental records; dotted curves, simulations. Experimental traces correspond to averages over (a) 4 shots and (b), (c), (d) 64 shots.

the chirp rate has never been low enough for the echo field to be truly given by the Fourier transform of the input signal, which is obvious from comparison of Figs. 3(d) and 2(b). It is the use of a collinear photon echo setup that prevented us from exploring lower chirp rates, because in this geometry the echo must be separated in time from the reading third pulse.

On the other hand, one may wonder about the behavior of the echo for higher chirp rates. In particular, because the input signal has a periodic pattern one may expect Talbot self-imaging effects. In the space domain the Talbot parameter when one is observing at distance d the diffraction pattern from a periodic mask with period p is $\lambda d/p^2$. For distances such that this parameter is an integer the original mask pattern is recovered, save for a π phase shift for odd integers. For half-integers, doubling of the input signal frequency is expected. In our experiment the Talbot parameter is $Q = 1/r\tau_m{}^2$, where $\tau_m = 200$ ns is the pulse-train period. We verified with the computer program used to simulate the echo signal that the expected self-imaging and frequency doubling effects should indeed be observed for $Q < 5$. For higher Q values the frequency doubling effect is no longer observed, and self-imaging becomes degraded because of increasing Fresnel number. The lowest Q value achieved in the experiment actually corresponds to $Q = 11/2\ r = 4.55$ MHz/μs, which unfortunately is too high for frequency doubling. The maximum chirp rate in the experiment was limited by the ramp generator driving both the AO1 and the AO2 cell. Higher chirp rates could easily be achieved with existing technology. Investigation of time–domain Talbot effects would then be possible.

To summarize, we have performed a photon-echo experiment in Tm^{3+}:YAG that showed for the first time to our knowledge the transition from Fresnel to Fraunhofer diffraction in the time domain. This experiment demonstrates the unequaled dispersion capability of the photon-echo process in rare-earth-doped crystals and opens the way to further investigation of space–time duality. In particular, this dispersion capability, characterized by the inverse of the chirp rate r, could be best if it were associated with the time lens such that the combination were a 1-f Fourier transformer.[15] As a matter of fact, chirping the signal at the opposite chirp rate, $-r$, gives the appropriate lens. Hence several photon-echo schemes can be designed for time-to-frequency Fourier transformation of rf optical signals.

The experimental part of this study was carried out in Lund, Sweden, under the European Community Training and Mobility of Researchers grant "Access to Large Scale Facilities," contract ERBFMGECT950020D G12. I. Lorgere's e-mail address is lorgere@lac.u-psud.fr.

References

1. T. Wang, H. Lin, and T. W. Mossberg, Opt. Lett. **20,** 2033 (1995).
2. K. D. Merkell and W. R. Babbitt, Opt. Lett. **23,** 528 (1998).
3. M. Tian, F. Grelet, I. Lorgeré, J.-P. Galaup, and J.-L. Le Gouët, J. Opt. Soc. Am. B **16,** 74 (1999).
4. B. Boggs, C. Greiner, T. Wang, H. Lin, and T. W. Mossberg, Opt. Lett. **23,** 1906 (1998).
5. B. Luo, U. Elman, S. Kröll, R. Paschotta, and A. Tropper, Opt. Lett. **23,** 442 (1998).
6. L. Ménager, I. Lorgeré, J.-P. Galaup, J.-L. Le Gouët, D. Dolfi, and J.-P. Huignard, presented at the Workshop of Applications of Spectral Hole Burning, Montana State University, Bozeman, Mont., March 8–11, 1998.
7. B. H. Kolner, IEEE J. Quantum Electron. **30,** 1951 (1994).
8. A. A. Godil, B. A. Auld, and D. M. Bloom, Appl. Phys. Lett. **62,** 1047 (1993).
9. M. T. Kauffman, W. C. Banyai, A. A. Godil, and D. M. Bloom, Appl. Phys. Lett. **64,** 270 (1994).
10. C. V. Bennett, R. P. Scott, and B. H. Kolner, Appl. Phys. Lett. **65,** 2513 (1994).
11. T. W. Mossberg, Opt. Lett. **7,** 77 (1982).
12. R. M. Macfarlane, Opt. Lett. **18,** 1958 (1993).
13. E. B. Treacy, IEEE J. Quantum Electron. **5,** 454 (1969).
14. M. V. Berry and S. Klein, J. Mod. Opt. **43,** 2139 (1996).
15. See, e.g., A. W. Lohmann and D. Mendlovic, Appl. Opt. **31,** 6212 (1992).